

The hcp-bcc transition of Be via anisotropy of modulus and sound velocity

Zhen Yang(杨真), Jia-Wei Xian(咸佳伟), Xing-Yu Gao(高兴誉), Fu-Yang Tian(田付阳), and Hai-Feng Song(宋海峰)
Citation: Chin. Phys. B, 2024, 33 (**11**): 116401. DOI: 10.1088/1674-1056/ad73b0
Journal homepage: http://cpb.iphy.ac.cn; http://iopscience.iop.org/cpb

What follows is a list of articles you may be interested in

K-core attack, equilibrium *K*-core, and kinetically constrained spin system

Hai-Jun Zhou(周海军)
Chin. Phys. B, 2024, 33 (**6**): 066402. DOI: 10.1088/1674-1056/ad4329

Pressure-induced magnetic phase and structural transition in $SmSb_2$

Tao Li(李涛), Shuyang Wang(王舒阳), Xuliang Chen(陈绪亮), Chunhua Chen(陈春华), Yong Fang(房勇), and Zhaorong Yang(杨昭荣)
Chin. Phys. B, 2024, 33 (**6**): 066401. DOI: 10.1088/1674-1056/ad362c

Comparative study on phase transition behaviors of fractional molecular field theory and random-site Ising model

Ting-Yu Liu(刘婷玉), Wei Zhao(赵薇), Tao Wang(王涛), Xiao-Dong An(安小冬), Lai Wei(卫来), and Yi-Neng Huang(黄以能)
Chin. Phys. B, 2024, 33 (**3**): 036403. DOI: 10.1088/1674-1056/ad0cc7

Spatial distribution order parameter prediction of collective system using graph network

Huimin Zhao(赵慧敏), Rui Wang(王瑞), Cai Zhao(赵偲), and Wen Zheng(郑文)
Chin. Phys. B, 2023, 32 (**5**): 056402. DOI: 10.1088/1674-1056/acb9fa

Stability of the topological quantum critical point between multi-Weyl semimetal and band insulator

Zhao-Kun Yang(杨兆昆), Jing-Rong Wang(王景荣), and Guo-Zhu Liu(刘国柱)
Chin. Phys. B, 2023, 32 (**5**): 056401. DOI: 10.1088/1674-1056/acbaf2

The hcp–bcc transition of Be via anisotropy of modulus and sound velocity

Zhen Yang(杨真)[1,2], Jia-Wei Xian(咸家伟)[2], Xing-Yu Gao(高兴誉)[2,†], Fu-Yang Tian(田付阳)[1,‡], and Hai-Feng Song(宋海峰)[2]

[1] *Institute of Applied Physics, University of Science and Technology Beijing, Beijing* 100083, *China*
[2] *National Laboratory of Computational Physics, Institute of Applied Physics and Computational Mathematics, Beijing* 100088, *China*

(Received 17 May 2024; revised manuscript received 9 August 2024; accepted manuscript online 27 August 2024)

Based on *ab initio* calculations, we utilize the mean-field potential approach with the quantum modification in conjunction with stress–strain relation to investigate the elastic anisotropies and sound velocities of hcp and bcc Be under high-temperature (0–6000 K) and high-pressure (0–500 GPa) conditions. We propose a general definition of anisotropy for elastic moduli and sound velocities. Results suggest that the elastic anisotropy of Be is more significantly influenced by pressure than by temperature. The pressure-induced increase of c/a ratio makes the anisotropy of hcp Be significantly strengthen. Nevertheless, the hcp Be still exhibits smaller anisotropy than bcc Be in terms of elastic moduli and sound velocities. We suggest that measuring the anisotropy in shear sound velocity may be an approach to distinguishing the hcp–bcc phase transition under extreme conditions.

Keywords: anisotropy, phase transition, elastic and sound properties, mean-field potential

PACS: 64.70.–p, 46.25.Hf, 46.40.–f, 46.25.Cc **DOI:** 10.1088/1674-1056/ad73b0

1. Introduction

Beryllium (Be) has only four electrons, the highest Debye temperature under ambient conditions in metals, the obviously anharmonic effect at high temperature, and the possible hcp–bcc phase transition at high pressure.[1] It is crucial in aircraft, aerospace, satellite, and nuclear energy industry applications, especially in extreme conditions, such as inertial confinement fusion (ICF) at extremely high temperature and high pressure.[2,3] Many experiments have been conducted on the elastic properties of Be under extreme conditions.[4–6] Brown *et al.* studied the change of shear modulus (G) in the range of 19–110 GPa under isotherm compression, while there is a significant uncertainty in this measurement.[5] McCoy *et al.* reported the moduli and sound velocities on Hugoniot from 90 to 190 GPa. They attempted to investigate the hcp–bcc phase transition, but the sound velocities do not show a noticeable mutation before melting on Hugoniot.[6]

To reveal the intrinsic properties of Be at high temperature and high pressure, various methods are employed to study the hcp–bcc phase transition. These methods include the quasi-harmonic approximation (QHA),[7] phonon quasiparticle method[8] and thermodynamic integration method.[9] The two latter methods have high accuracy, but they face a large number of calculations. Recently, machine learning has been used to study phase transitions, which can greatly reduce research costs.[10] The comparison results indicate that the anharmonic effect is crucial in the study of properties of Be at high temperature.[3,8,11,12] Robert *et al.* proposed the full QHA to study the temperature-dependent elastic moduli of Be at ambient pressure and its sound velocities on Hugoniot.[7] The sound velocities of hcp Be align with the available experiments, whereas the sound velocities of bcc on Hugoniot deviated from the experiments of McCoy *et al.*[6,7] This discrepancy may be due to the strong anisotropy of sound velocities under extreme conditions.

Sound velocities can be used to understand physical properties of materials under extreme conditions and to bridge the theoretical and experimental investigations. For instance, Antonangeli *et al.* obtained the anisotropic sound velocities of hcp-iron (Fe) at 22 GPa and 112 GPa at room temperature using the inelastic x-ray scattering (IXS) in a diamond anvil cell (DAC).[13] The anisotropy in sound velocity of Fe at high pressure sheds light on different propagation velocities of sound waves on Earth's core, as reported by Belones *et al.*, based on the calculated sound velocities as a function of direction for hcp and bcc Fe.[14] With the sound velocities, ones can estimate the moduli at high pressure. Although the sound velocities and moduli are theoretically derived from the elastic constants, their anisotropies are obviously different. To our best knowledge, there are limited reports on the modulus and sound velocity anisotropy of Be.[15–18] Kádas *et al.* suggested that the significant difference in elastic anisotropy A_{VR} could be used to study the hcp–bcc phase transition.[18] However, the general parameter of anisotropy measured in experiments is still lacking.[18,19] More importantly, it is necessary to calculate the moduli and sound velocities as functions of direction

†Corresponding author. E-mail: gao_xingyu@iapcm.ac.cn
‡Corresponding author. E-mail: fuyang@ustb.edu.cn

© 2024 Chinese Physical Society and IOP Publishing Ltd

and to study the change of anisotropy versus high temperature and high pressure.

In this work, we utilize the mean-field potential (MFP)[20–24] with new quantum modification (QM)[25] in combination with the first principles calculations to study the elastic properties and sound velocities of both hcp and bcc Be under extreme conditions. We propose the generally anisotropic indicator at high temperature and pressure. Furthermore, we examine the impact of pressure and temperature in anisotropies of modulus and sound velocity. We find that the pressure has a significant affect on the anisotropies of modulus and sound velocity. The anisotropy of bcc Be is more pronounced but less sensitive to the pressure and temperature, compared to hcp Be. Unlike the moduli, the anisotropy in longitudinal sound velocity of bcc Be is inapparent due to the opposite anisotropy between Young's modulus (E) and G. More importantly, it may be worth investigating the anisotropy of shear sound velocities to distinguish the hcp–bcc phase transition.

2. Method

We obtained the volume-dependent energies, electronic properties, and elastic constants of hcp and bcc Be from first-principles calculations at $T = 0$ K and $P = 0$–500 GPa. In the present calculations implemented in the Vienna *ab initio* Simulation Package (VASP),[26] the exchange–correlation potentials were treated by the Perdew–Burke–Ernzerhof (PBE) functional. The electron–ion interaction was described by the projector augmented wave (PAW) method. The plane-wave cutoff energy is 600 eV. The Brillouin zone sampling was performed by the Monkhorst–Pack scheme with $37 \times 37 \times 25/33 \times 33 \times 33$ k-mesh for the hcp/bcc structure. The convergence tolerance level is 10^{-6} eV for total energy and 0.01 eV/Å for the maximum force on each atom. In the framework of stress–strain relation, the elastic constants were obtained by using the first principles in combination with elastic deformation matrix proposed by Jian *et al.*[27]

The calculated static energies and characteristic temperatures derived from the 0-K phonon moments are used to construct the MFP[20–24] with QM.[25] The phonon moments were calculated based on the phonon density of states by using the phonopy.[28] By utilizing the MFP with QM, we obtained the ionic part of the Helmholtz free energy. This method not only describes the quantum effect at low temperature, but also takes into account the anharmonic influence at elevated temperature. The electronic contribution was calculated from 0 K electronic density of state by Mermin statistics.[29] Using the summation of static energy, ionic and electronic parts, we arrive at the multiphase equation of state of solid Be. Notably the phase boundaries in the P–T diagram are from the results of Robert *et al.* (melting curve) and Xian *et al.* (hcp–bcc boundary).[7,8]

Based on elastic constants at zero temperature, we combined the quasi-static approximation (QSA)[30] with the MFP method to estimate the elastic properties and sound velocities at high temperature. The anisotropic thermal expansion coefficients and specific heat at high pressure and high temperature were calculated in the framework of MFP. The isothermal elastic constants were obtained via the QSA approach. By combining the thermal properties with isothermal elastic constants, we could get the isentropic elastic constants, anisotropic elastic moduli and sound velocities at $P = 0$–500 GPa and $T = 0$–6000 K. According to the elasticity theory,[31,32] we could obtain the elastic moduli and sound velocity anisotropy as functions of temperature and pressure. Table S1 and Fig. S1 in the supplementary material (SM) show our calculated zero temperature elastic constants and elastic moduli for hcp and bcc Be in the range of 0–500 GPa, respectively. To validate our approach, we also calculated the isentropic elastic constants of hcp Be at room temperature (300 K) and elastic moduli. Our results are in good agreement with experiments.

3. Results and discussion

Considering that the anisotropy of B depends on E and G, we only study the anisotropy of E and G in the present work. Figure 1 shows E and G along the crystal directions or planes and the anisotropy diagram of solid Be across a wide P–T range. The Miller indices (normal direction of the crystal plane) are chosen as the direction. E depends on the crystal plane and crystalline direction equivalently, while G is dependent on different crystal planes. We also show the 3D Young's modulus (see Fig. S2 in SM). Therefore, the Miller indices are appropriate to represent the dependence of directions for both E and G.

For hcp and bcc Be, both E and G show a significant change on different crystal planes. Walsh *et al.*[16] and Kuksenko *et al.*[17] measured the change of E with directions for polycrystalline hcp Be from 287 (275) GPa to 341 (340) GPa at ambient pressure. Our calculated E of single crystalline hcp Be is from 275 GPa to 333 GPa. Considering the uncertainty of measurement, experimental results are consistent with our single-crystalline E. For the polycrystalline materials, the measured E is an average value. The largest E of bcc Be is on (111) planes, while the smallest G is on (111) planes. The opposite case also occurs on (001) planes. Compared with bcc Be, the anisotropic value of hcp Be is smaller. While the elastic anisotropy is more sensitive to pressure for hcp Be, it derives from the change of structural parameter c/a (see Fig. S3 in SM). With the pressure increasing to 400 GPa, the c/a ratio changes from 1.575 to 1.620. We note that for hcp Be the elastic anisotropy indicated by E and G becomes stronger as c/a ratio approaches the ideal axial ratio (see Fig. S3 in SM).

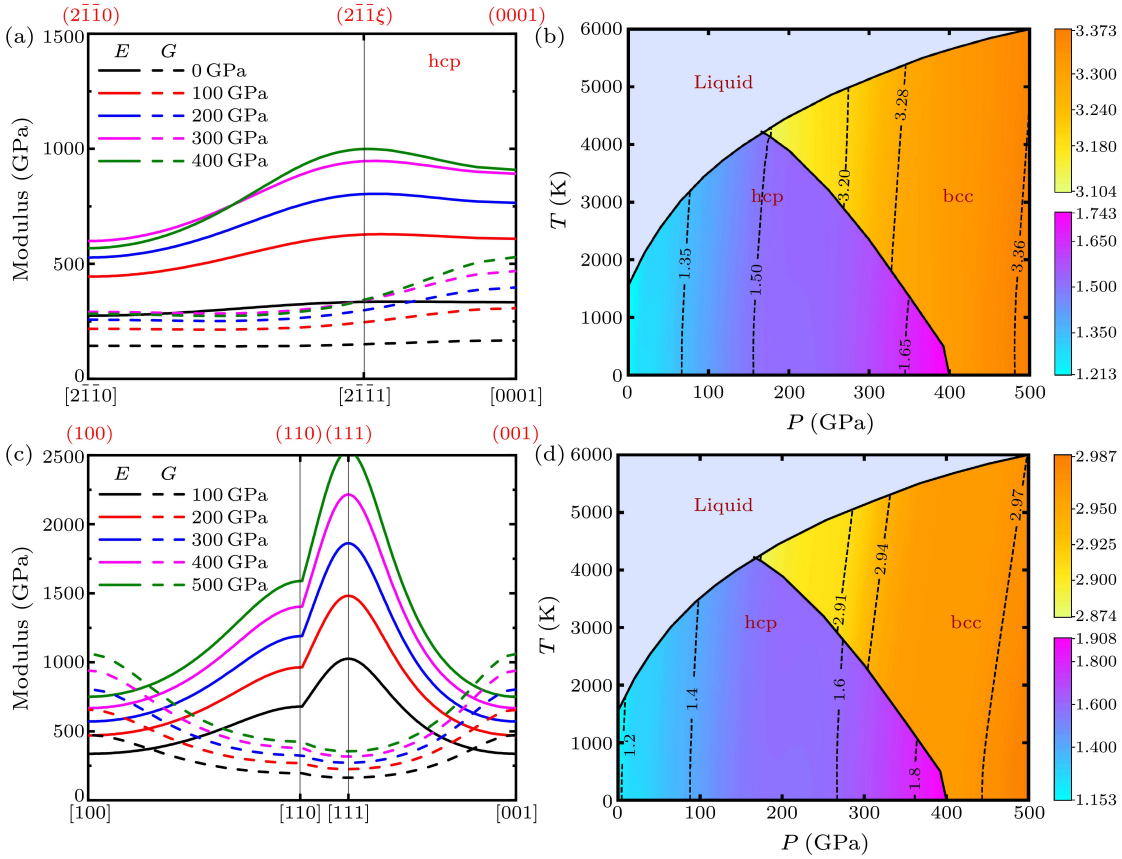


Fig. 1. Pressure-dependent Young's modulus E and shear modulus G at 0 K for hcp (a) (0–400 GPa) and bcc (b) (100–500 GPa) phase (Here $\xi = 2c/a$ for hcp structure). The anisotropy diagram of Δ_E (c) and Δ_G (d) for hcp and bcc Be in the ranges of pressure (0–500 GPa) and temperature (0–6000 K).

Many anisotropic parameters were proposed to quantify the anisotropy of modulus. Zener's ratio $A_Z = 2C_{44}/(C_{11} - C_{12})$[31] and Every's ratio $A_E = (C_{11} - C_{12} - 2C_{44})/(C_{11} - C_{44})$[32] are only proper to describe the intrinsic anisotropy of cubic lattice, for instance, bcc Be. The two other indicators $A_{VR} = (G_V - G_R)/(G_V + G_R)$[19] and $A_U = 5(G_V/G_R) + B_V/B_R - 6$[33] are derived from the G and B of Voigt and Reuss bounds. These anisotropic indicators do not suggest the change of E and G moduli along crystalline direction. Herein we define the simple ratio parameters ($\Delta_E = E^{max}/E^{min}$ and $\Delta_G = G^{max}/G^{min}$) to describe the anisotropy of elastic moduli ($\Delta = 1$ means the isotropy). The anisotropic parameters Δ_G, A_{VR}, A_U and A_Z have almost identical trends with the increasing pressure (see Table S2 and Fig. S4 in the SM). Such as hcp Be, A_U has a slope of ten times than A_{VR} in the range of 0–500 GPa, and Δ_G has a slope of 3.7 times than A_U. As for the bcc Be, the slopes between Δ_G, A_{VR}, A_U, and A_Z are also multiple relationships. This is due to fact that these parameters are mainly derived from the shear elastic properties, but they are weak to describe the anisotropy of Young's modulus.

The diagrams of modulus anisotropy under extreme conditions are further shown in Figs. 1(c) and 1(d). Because of the strong dependence of crystal plane, the bcc Be shows at least 1.4- and 1.8-times anisotropy of E and G than hcp at the hcp–bcc phase boundary. Meanwhile, the maximum difference of B between two phases is at most 1%, and both differences between two phases for E and G are not more than 10% at the hcp–bcc phase boundary. In contrast, the difference of anisotropy between two phases is apparent. The anisotropy of E and G is 1.5–1.7 and 1.5–1.9 for hcp at phase boundary, and the anisotropy of E and G is 3.1–3.4 and 2.9–3.0 for bcc. In addition, the anisotropy of E and G is less sensitive to the temperature at different pressures for both hcp and bcc Be. The increase of temperature slightly hinders the anisotropy. In contrast, the increase of pressure obviously strengthens the elastic anisotropy at different temperatures. The anisotropy of E and G in hcp depends more on pressure than that in bcc Be at different temperatures.

Figure 2 shows longitudinal and shear sound velocities v_l, v_{s1}, and v_{s2} along different propagation directions at wide pressures for hcp and bcc Be. We find from Fig. 2(a) that the direction of minimum v_l is along [2$\bar{1}\bar{1}$0] with $\theta_z = 90°$ (θ_z is the angle from the z axis) at 0 GPa, while the minimum direction of propagation is monotonically changed to $\theta_z = 60°$ at 400 GPa. The change of propagation direction leads to that Steinle–Neumann's parameters[34] ($\Delta_l = [v_l([0001])/v_l([2\bar{1}\bar{1}0])]^2 = C_{33}/C_{11}$, $\Delta_{s1} = [v_{s1}(\theta_z = 45°)/v_{s1}([2\bar{1}\bar{1}0])]^2 = [C_{11} + C_{33} - 2C_{13}]/4C_{44}$ and $\Delta_{s2} = [v_{s2}([0001])/v_{s2}([2\bar{1}\bar{1}0])]^2 = C_{44}/C_{66}$) are insufficient to well describe the anisotropy of longitudinal sound velocities for hexagonal systems at high pressures. We

note that the anisotropy of sound velocity $A^* = (v_s^{max}/v_s^{min})^2$ proposed by Ledbetter *et al.* has been used to distinguish the anisotropic properties between the hexagonal and cubic systems.[35] However, this parameter is only applicable to shear sound velocity and does not distinguish between different branches of sound velocities.[34] We propose a universal form ($\Delta_l = (v_l^{max}/v_l^{min})^2$, $\Delta_{s1} = (v_{s1}^{max}/v_{s1}^{min})^2$, and $\Delta_{s2} = (v_{s2}^{max}/v_{s2}^{min})^2$) to describe the anisotropy of sound velocities ($\Delta = 1$ means isotropy). This form can give the almost same anisotropy parameters as Steinle–Neumann's parameters[34] at 0 GPa, also our definition can excellently distinguish the longitudinal and shear sound velocities at different pressures [see Eqs. (S6)–(S10) in the SM for detailed analysis].

Figure 3 shows the anisotropic diagrams of longitudinal and shear sound velocities. The trend of anisotropy with temperature and pressure is similar to the case of moduli. Notably, the bcc Be is slightly anisotropic in longitudinal sound velocity, whereas its E and G keep a strong anisotropy. This is attributed to the opposite trends of E and G in the different directions of planes. The anisotropy of longitudinal sound velocity for bcc phase is not obviously more significant than that of hcp Be. However, Fig. 3 shows the large difference in anisotropy of shear sound velocity between hcp and bcc Be. It could be worth trying to distinguish the phase transition by the measurements on anisotropy of shear sound velocities. Beason *et al.* have reported that the measurement of sound velocities in Hugoniot experiments is used to clear the phase transition for magnesium during the shock compression process. However, the difference in sound velocities between hcp and bcc is not apparent.[36] A similar case could occur for Be because the sound velocity is not mutated on Huogoniot in experiments, and the theoretical calculations of sound velocities are very close for the bcc and hcp phases.

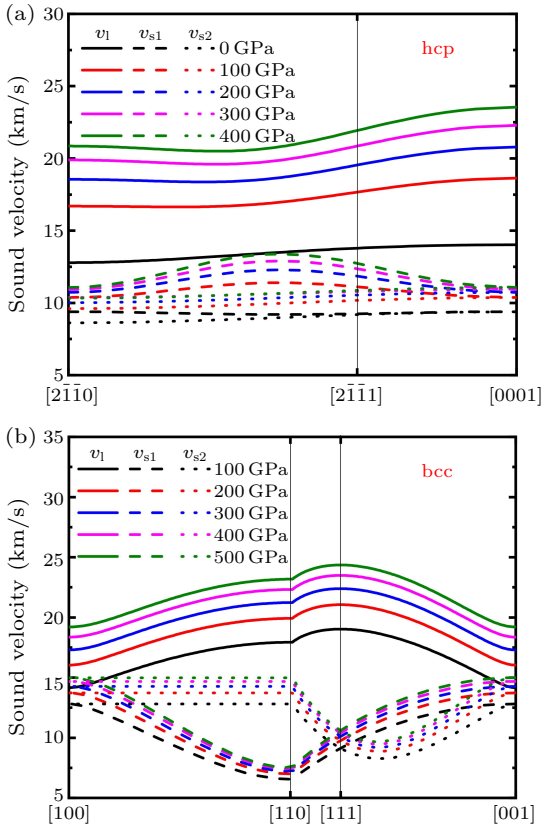


Fig. 2. Pressure-dependent longitudinal (v_l) and shear sound velocities (v_{s1} and v_{s2}) along different propagation directions at 0 K for hcp (a) (0–400 GPa) and bcc (b) (100–500 GPa) phases. Two branches s1 and s2 of shear sound velocities are along different polarization directions (s1 is polarized perpendicular to basal plane while s2 is polarized in the basal plane.[34]

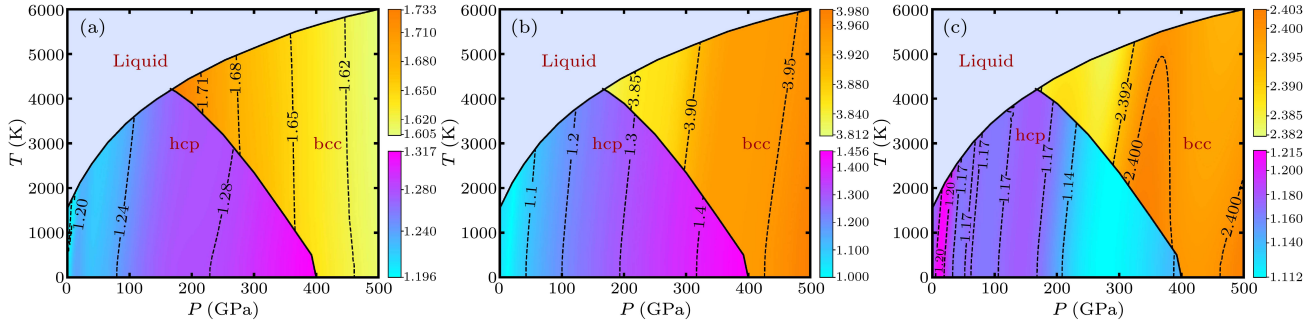


Fig. 3. Anisotropy of longitudinal (Δ_l) (a) and shear (Δ_{s1} and Δ_{s2}) [(b), (c)] sound velocities for hcp and bcc in the ranges of pressure (0–500 GPa) and temperature (0–6000 K).

Figure 4 shows our calculated hcp (0–203 GPa), bcc (180–215 GPa) T–P, P–ρ and v_l–P (v_b-P) relationships on Hugoniot. Our Hugoniot T–P relationships of both hcp and bcc Be are in good agreement with the results of McCoy *et al.*[6,37] Our P–ρ results of the two phases are almost all within the experimental errors.[6,37] We find that the density could not be used to differentiate hcp–bcc transition due to the close density and temperature near the phase transition pressure.

Our calculated sound velocities of hcp and bcc Be are close to the experimental results at pressure $P < 150$ GPa.[6,7] Above 150 GPa, the experimental longitudinal sound velocity of McCoy *et al.* rapidly decreases with increasing pressure and is close to the bulk sound velocity of about 201 GPa. This process could be considered as shock melting process and the solid-liquid mixture could be in such a range.[7,38] The max difference between two phases is less than 0.5 km/s for all theoretically sound velocities, which is much smaller than the measurement error (1 km/s) given by the experiment.[6,7] This

means that there is no sudden change in sound velocities on Hugoniot around phase boundary. It is challenging to validate the phase transition by directly measuring sound velocities.

Figure 5 shows the longitudinal and shear sound velocities, and their upper and lower limits at isotherms. Here the upper limit and lower limit mean the maximum and minimum sound velocities for the direction-dependent sound velocity. The interval of direction-dependent sound velocity could help us to understand the discrete values of sound velocities from the static high-pressure experiment for the polycrystal material. As discussed on Young's modulus along crystalline direction, our predicted interval of elastic modulus covers the measured results.

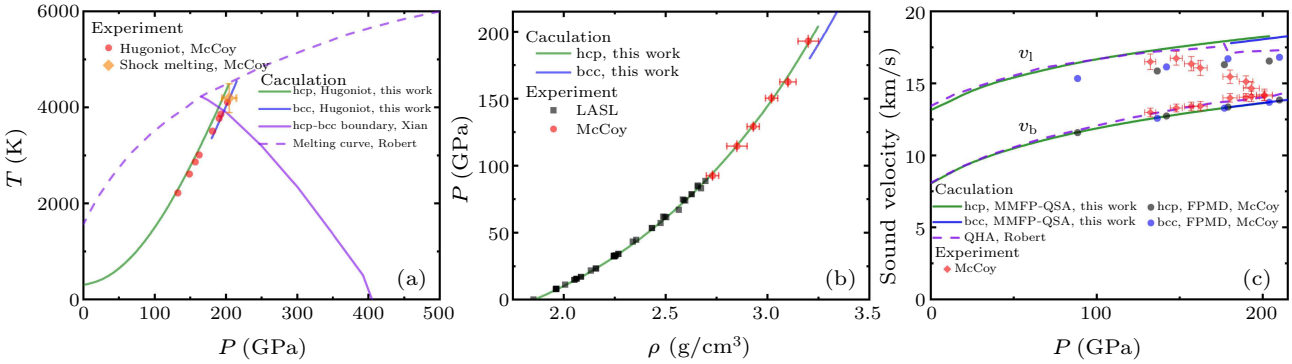


Fig. 4. Hugoniot properties including (a) Hugoniot T–P relationship, (b) Hugoniot P–ρ relationship, and (c) Hugoniot sound velocities at $P = 0$–215 GPa.

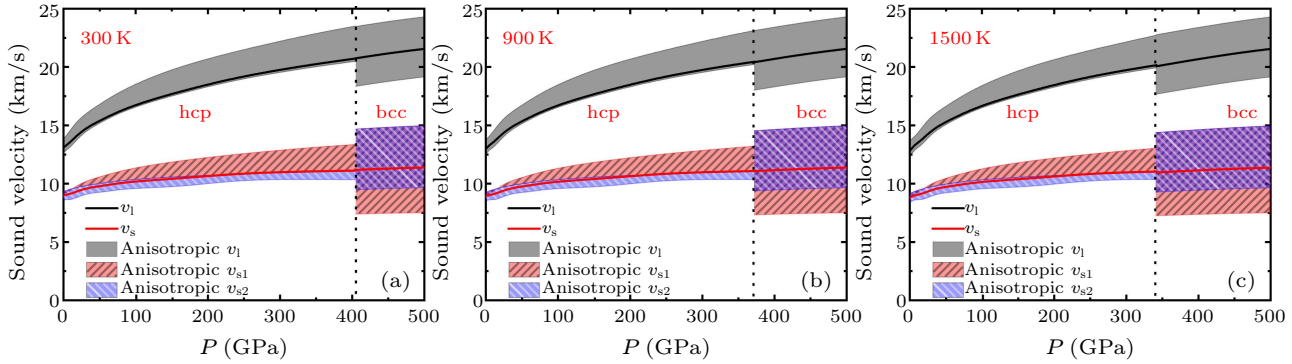


Fig. 5. Longitudinal and shear sound velocities versus pressure, and their upper and lower limits for hcp and bcc Be at (a) 300 K, (b) 900 K, and (c) 1500 K isotherm. The black and red solid (dashed) lines represent the sound velocities of hcp (bcc) Be. The colored unshaded and shaded intervals are the ranges of the direction-dependent sound velocity. The vertical dashed line stands for the pressure of phase transition.

When the phase transition happens at high pressure for Be, the sound velocities do not significantly change (not exceeding 1%). By measuring longitudinal and shear velocities, it is difficult to distinguish the hcp–bcc phase transition. However, the shear sound velocity has a large anisotropy change between hcp–bcc transition (the bcc's Δ_{s1} and Δ_{s2} are at least 1.9 times than those of hcp). The upper and lower limits of the shear sound velocities at phase transition are significantly different. It could be worth trying to measure the anisotropy of shear sound velocity to distinguish the phase transition at high temperature and high pressure. This method has been shown to work under static high-pressure experiments. For example, Mao *et al.*[39] obtained the direction-dependent sound velocity at $P = 39$ GPa and 211 GPa for single-crystal iron, and Antonangeli *et al.*[13] found the anisotropy difference at two pressures $P = 22$ GPa and 112 GPa, via measuring the sound velocities along two crystal directions. Accordingly, we speculate that the sound velocities along different crystal directions could show the enormous change near the phase boundary of hcp–bcc. It means that we could compare measurements in different directions, or multiple sets of measurements to study the phase boundary in experiments. Meanwhile, it could help us to understand the discrete values of sound velocities for the polycrystal material.

4. Conclusion

In summary, based on first-principles calculations of a wide pressure range, we have combined the MFP with QM and QSA to study the elastic properties under extreme conditions ($T = 0$–6000 K and $P = 0$–500 GPa). A general indicator of anisotropy is proposed for elastic modulus and sound velocity. We find that bcc Be exhibits a greater anisotropy than hcp in terms of the E and G moduli and sound velocities. The anisotropies in both the modulus and sound velocity of hcp Be are more sensitive to pressure because of the change of c/a induced by compression. Additionally, the opposite trends of

E and *G* in different crystal planes of bcc Be result in smaller anisotropy in longitudinal sound velocities. We observe that the compression enhances the anisotropy in both modulus and sound velocity, while the temperature has a slight inhibitory effect on the elastic anisotropy. The significant difference in shear sound velocity anisotropy between hcp and bcc Be suggests that measuring the sound velocities anisotropy of Be under extreme conditions such as Hugoniot may help distinguish the hcp–bcc transition.

Supplementary material

See the supplementary material for the calculated elastic constants and moduli, as well as a comparison of some anisotropic parameters and anisotropy phase diagram and analysis of extreme directions in sound velocities.

Acknowledgments

This work was supported by the National Natural Science Foundation of China (Grant Nos. U23A20537, U2230401, and 52371174) and Funding of National Key Laboratory of Computational Physics.

References

[1] Migliori A, Ledbetter H, Thoma D J and Darling T W 2004 *J. Appl. Phys.* **95** 2436
[2] Zheng L F, Wang X G, Yue L N, Xie Y J, Wu B P and Zhong J M 2020 *Mater. Sci. Forum.* **977** 261
[3] Wu C J, Myint P C, Pask J E, Prisbrey C J, Correa A A, Suryanarayana P and Varley J B 2021 *J. Phys. Chem. A* **125** 1610
[4] Lazicki A, Dewaele A, Loubeyre P and Mezouar M 2012 *Phys. Rev. B* **86** 174118
[5] Brown J L, Knudson M D, Alexander C S and Asay J R 2014 *J. Appl. Phys.* **116** 033502
[6] McCoy C A, Knudson M D and Desjarlais M P 2019 *Phys. Rev. B* **100** 054107
[7] Robert G, Legrand P and Bernard S 2010 *Phys. Rev. B* **82** 104118
[8] Xian J W, Yan J, Liu H F, Sun T, Zhang G M, Gao X Y and Song H F 2019 *Phys. Rev. B* **99** 064102
[9] Wu J, González-Cataldo F and Militzer B 2021 *Phys. Rev. B* **104** 014103
[10] Ma Y G, Pang L G, Wang R and Zhou K 2023 *Chin. Phys. Lett.* **40** 122101
[11] Wu J, González-Cataldo F, Soubiran F and Militzer B 2022 *J. Phys.: Condens. Matter* **34** 144003
[12] Lu Y, Sun T, Zhang P, Zhang P, Zhang D B and Wentzcovitch R M 2017 *Phys. Rev. Lett.* **118** 145702
[13] Antonangeli D, Occelli F, Requardt H, Badro J, Fiquet G and Krisch M 2004 *Earth Planet. Sci. Lett.* **225** 243
[14] Belonoshko A B, Skorodumova N V, Rosengren A and Johansson B R 2008 *Science* **319** 797
[15] Luo F, Cai L C, Chen X R, Jing F Q and Alfè D 2012 *J. Appl. Phys.* **111** 053503
[16] Walsh K A 2009 *Beryllium Chemistry and Processing* (ASM International)
[17] Kuksenko V, Roberts S and Tarleton E 2019 *Int. J. Plast.* **116** 62
[18] Kádas K, Vitos L, Johansson B and Kollár J 2007 *Phys. Rev. B* **75** 035132
[19] Anderson O L 1963 *J. Phys. Chem. Solids* **24** 909
[20] Wang Y, Chen D and Zhang X 2000 *Phys. Rev. Lett.* **84** 3220
[21] Wang Y, Ahuja R and Johansson B 2004 *Int. J. Quantum Chem.* **96** 501
[22] Li L and Wang Y 2001 *Phys. Rev. B* **63** 245108
[23] Song H and Liu H 2007 *Phys. Rev. B* **75** 245126
[24] Song H, Tian M, Liu H, Song H and Zhang G 2014 *Chin. Phys. Lett.* **31** 016402
[25] Gao X, Yang Z, Fang J, Xian J, Liu H and Song H *A multiphase fast previewer based on mean-field potential approach: Beryllium as a prototype* (in preparation)
[26] Kresse G and Furthmüller J 1996 *Comput. Mater. Sci.* **6** 15
[27] Jian D, Zhu X, Liu Y, Song H and Lai X 2021 *Mater. Rep.* **35** 1082 (in Chinese)
[28] Togo A and Tanaka I 2015 *Scr. Mater.* **108** 1
[29] Mermin N D 1965 *Phys. Rev.* **137** A1441
[30] Wang Y, Wang J J, Zhang H, Manga V R, Shang S L, Chen L Q and Liu Z K 2010 *J. Phys.: Condens. Matter* **22** 225404
[31] Zener C 1948 *Phys. Rev.* **74** 639
[32] Every A 1980 *Phys. Rev. B* **22** 1746
[33] Ranganathan S I and Ostoja-Starzewski M 2008 *Phys. Rev. Lett.* **101** 055504
[34] Steinle-Neumann G, Stixrude L and Cohen R E 1999 *Phys. Rev. B* **60** 791
[35] Ledbetter H and Migliori A 2006 *J. Appl. Phys.* **100** 063516
[36] Beason M T, Jensen B J and Crockett S D 2021 *Phys. Rev. B* **104** 144106
[37] Marsh S P 1980 *LASL Shock Hugoniot Data* (University of California Press) **5** p. 21
[38] Tan H 2018 *Experimental Shock Wave Physics* (Beijing: National Defense Industry Press) p. 177
[39] Mao H K, Shu J, Shen G, Hemley R J, Li B and Singh A K 1998 *Nature* **396** 741